Supplementary Materials

This document provides the supplementary materials for the paper "An Optimal Control Approach to Identify the Worst-Case Cascading Failures in Power Systems" by Chao Zhai, Hehong Zhang, Gaoxi Xiao, and Tso-Chien Pan. It aims to demonstrate the validity of the proposed model and the optimal control approach through the validation with other cascading failure models (e.g. the COSMIC model), the comparison with the AC power flow model, and the consideration of protective actions (i.e. generation dispatch and load shedding).

1 Validation with the COSMIC model

It is feasible to validate the cascade sequence with other cascading failure models. To see the consistency or discrepancy, we validate the cascade sequence on the IEEE 39 Bus System by using the Cascading Outage Simulator with Multiprocess Integration Capabilities (COSMIC) model [1], which is able to allow for a wide variety of cascading outage mechanisms (e.g. machine dynamics, protective relays, AC power flow, load types, etc). For a fair comparison, the threshold of branches in the COSMIC model is the same as that in our model in the paper (i.e. the threshold of active power flow on each branch is 10% larger than their respective active power flow in the normal condition without any disturbances). And the branch is severed if its active power flow is larger than the given threshold. Matlab R2010a is adopted to run the codes of the two cascade models. To quantitatively compare the line outage sequences of the two models, the index of path agreement is introduced as follows [1, 2]:

$$\eta = \frac{|A \cap B|}{|A \cup B|} \in [0, 1] \tag{1}$$

where A and B denote the sets of outage branches using the COSMIC model and our DC model, respectively. In addition, $|A|$ refers to the cardinality of the set A (i.e. the number of members of

A). Essentially, the index η is the ratio of the same outage branches over the total outage branches for both models. And a larger value of η indicates a better match between the results given by the two models. As reported by the proposed approach (see Table II on Page 8 of the paper), the most disruptive disturbance is to sever Branch 35 at the initial cascading step. Thus Branch 35 is severed as the triggering event for both the COSMIC model and our DC model, which directly initiates the chain reactions of branch outages for the two models. As for the index of path agreement, we have $\eta = 1$ for the first 3 branch outages and $\eta = 0.67$ for the first 10 branch outages, which implies the desirable path agreement in the early stage of cascades. For the first 3 branch outages, the sets of branch ID are $\{21, 35, 36\}$ for the two models. For the first 10 branch outages, the sets of branch ID are $\{1, 2, 3, 7, 19, 20, 21, 25, 35, 36\}$ for the COSMIC model and $\{2, 3, 7, 8, 19, 21, 25, 29, 35, 36\}$ for our DC model, respectively. In terms of the whole branch outages, the sets of branch ID are $\{1, 2, 3, 4, 5, 6, 7, 8, 14, 15, 19, 20, 21, 25, 26, 35, 36, 44\}$ for the COSMIC model and $\{2, 3, 4, 7, 8, 13, 14, 16, 17, 18, 19, 21, 22, 23, 24, 25, 27, 29, 31, 33, 34, 35, 36, 38, 40, 42\}$ for our DC model, respectively. It is worth pointing out that the COSMIC model stops the cascading evolution after 18 branch outages due to the non-convergence of numerical algorithms. Thus, we obtain $\eta = 0.33$ for the whole branch outages, which indicates the discrepancy of branch outage path between the two cascade models after the early stage of cascades. This discrepancy in line outage paths during later stages is partly due to the fact that our DC model tends to produce longer cascades without reliable protection actions, which increases the denominator in Equation (1) [1]. The COSMIC model allows for more physical characteristics of real power systems, and it is expected to produce more realistic path of branch outages in spite of its instability of numerical algorithms. Although the worst cases are not exactly the same in terms of branch outages for the two models, the path agreement of branch outages in the early stage provides insights into the identification of initial disruptive disturbances in the real power systems.

Note that the cascading failure path after the early stage is notoriously difficult to predict as many factors can change the progress of cascades. Seldom any two simulators, if not never, could manage to steadily generate similar results for late-stage developments of cascading failure. Nevertheless, we may observe that a worst initial disturbance for one model (e.g. the DC model) turns out to be a very bad, though not necessarily the strictly worst, initial disturbance for the other (e.g. the COSMIC model). That is encouraging though further studies are needed

to better understand the late-stage developments of a cascading failure.

2 Comparison between AC and DC power flow models

In this section, we compare the proposed DC model with the AC power flow model on IEEE 9 Bus System (see Fig. 1 and Fig. 2). The vector of power flow threshold on each branch is $c = (c_{ij}) = (1, 1.8, 1, 0.6, 0.5, 1, 1, 1, 1)$, and other parameter setting is the same as that for IEEE 14 Bus System in the paper. Specifically, Branch 2 is selected to add the initial disturbance (1.22), which is obtained by solving the proposed optimal control problem (6) in the paper. The initial disturbance does not sever Branch 2 immediately, but it results in the overload of Branch 2, which causes the branch outage. By adding the same initial disturbance on Branch 2, the cascading processes of both models are the same in terms of network topology and power flow direction at the first three cascading steps. Nevertheless, the final network topology of power system with the DC model is slightly different from that with the AC model at the fourth cascading step. To be precise, Branch 9 is severed with the DC model in Fig. 1, while it is still connected with the AC model in Fig. 2. As is known, the DC power flow is a linearization of the AC power flow under some assumptions [3], and the cascading process with the AC power flow is basically more realistic.

The DC model enables us to directly compute the power flow on high-voltage transmission lines by solving a system of linear equations. In comparisons, the numerical algorithm might not converge due to the nonlinearity and non-convexity of the AC model. Actually, the differences between the two models at the fourth cascading step in Fig. 1 and Fig. 2 mainly result from the non-convergence of numerical algorithm for the AC model. Thus, the DC model is a good substitute for the AC model for the high-voltage electric transmission system. Figure 3 presents the mismatches of power flow on each branch between the DC model and the AC model at different cascading steps. As we can see, the mismatch of power flow are relatively small (less than 0.1 pu) on all branches at the first two cascading steps (i.e. Step 1 and Step 2). At Step 3, the power flow mismatches become relatively large on Branch 3, Branch 6, Branch 7 and Branch 9 (more than 0.2pu) due to the divergence of numerical algorithm for the AC power flow equation. Finally, the mismatches of power flow become zero on all branches at Step 4.

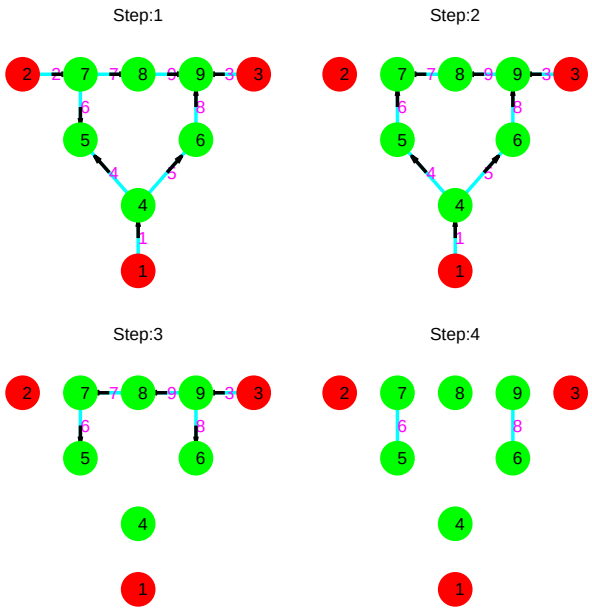

Figure 1: Cascading process of IEEE 9 Bus System with the DC power flow model.

3 Consideration of generation dispatch/load shedding

If generation dispatch/load shedding is taken into account in the proposed formulation, P^k has to be updated at certain steps of cascading failure. For simplicity, suppose that load shedding and generation control are implemented at the l-th cascading step ($1 < l < n$). This implies that $P^k = P^0$ for $k < l$ and $P^k = P^l$ for $k \geq l$, where P^0 denotes the vector of original injected power on buses. Thus, an optimization formulation can be proposed to allow for load shedding and generation control as follows

$$\begin{aligned} &\min_{P^l} \|P^l - P^0\|^2 \\ s.t. \quad &\underline{P}_i \leq P_i^l \leq \bar{P}_i \\ &-c_{ij} \leq P_{ij}^l \leq c_{ij} \end{aligned} \tag{2}$$

where $P^l = (P_1^l, P_2^l, ..., P_m^l)^T$ and $P_{ij}^l = e_i^T Y_b^l e_j (e_i - e_j)^T (Y_b^l)^{-1^*} P^l$. In addition, $\underline{P}_i$ and $\bar{P}_i$ denote the upper and lower bounds of injected power on Bus i, respectively. The cost function quantifies the changes of injected power on buses due to load shedding and generation control. The optimization objective is to achieve the optimal adjustment of injected power on buses to prevent the cascading outages of power grids. It is worth pointing out that the linear programming

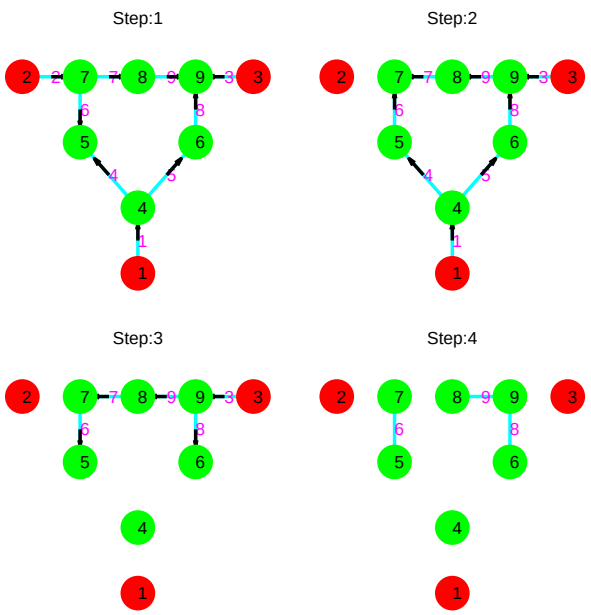

Figure 2: Cascading process of IEEE 9 Bus System with the AC power flow model.

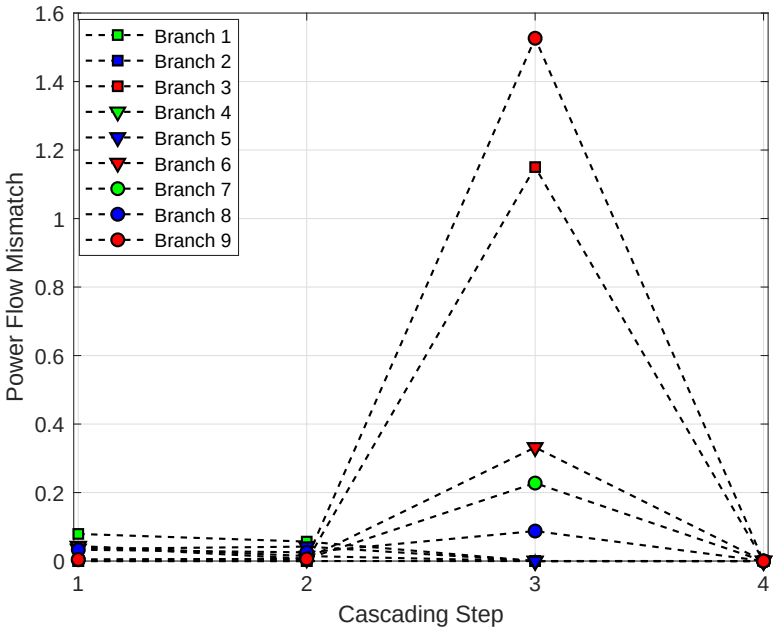

Figure 3: Power flow mismatch on each branch of the IEEE 9 Bus System at different cascading steps.

formulation can also be adopted to allow for protection actions in power systems [4].

Essentially, the inequality constraints in the optimization problem (2) can be converted into the equality constraints by introducing the unknown variables $\bar{x}_i$, $\underline{x}_i$, $\bar{y}_{ij}$ and $\underline{y}_{ij}$ as follows.

$$\begin{aligned} &\min_{P^l} \|P^l - P^0\|^2 \\ s.t. \quad & P_i^l - \bar{P}_i + \bar{x}_i^2 = 0 \\ & \underline{P}_i - P_i^l + \underline{x}_i^2 = 0 \\ & P_{ij}^l - c_{ij} + \bar{y}_{ij}^2 = 0 \\ & P_{ij}^l + c_{ij} - \underline{y}_{ij}^2 = 0 \end{aligned} \tag{3}$$

According to the Karush-Kuhn-Tucker (KKT) conditions, the necessary condition for the above optimization problem (3) are given by

$$\begin{aligned} & 2(P^l - P^0) + \bar{\mu} - \underline{\mu} + \sum_{(i,j)\in\Omega} (\bar{\lambda}_{ij} - \underline{\lambda}_{ij}) e_i^T Y_b^l e_j (Y_b^l)^{-1^*} (e_i - e_j) = 0_m \\ & P_i^l - \bar{P}_i + \bar{x}_i^2 = 0, \qquad \bar{\mu}_i (P_i^l - \bar{P}_i) = 0, \qquad \bar{\mu}_i - \bar{z}_i^2 = 0 \\ & \underline{P}_i - P_i^l + \underline{x}_i^2 = 0, \qquad \underline{\mu}_i (P_i^l - \underline{P}_i) = 0, \qquad \underline{\mu}_i - \underline{z}_i^2 = 0, \quad i \in I_m \\ & P_{ij}^l - c_{ij} + \bar{y}_{ij}^2 = 0, \quad (P_{ij}^l - c_{ij}) \bar{\lambda}_{ij} = 0, \quad \bar{\lambda}_{ij} - \bar{w}_{ij}^2 = 0 \\ & P_{ij}^l + c_{ij} - \underline{y}_{ij}^2 = 0, \quad (P_{ij}^l + c_{ij}) \underline{\lambda}_{ij} = 0, \quad \underline{\lambda}_{ij} - \underline{w}_{ij}^2 = 0, \quad (i,j) \in \Omega \end{aligned} \tag{4}$$

where $\bar{\mu} = (\bar{\mu}_1, \bar{\mu}_2, ..., \bar{\mu}_m)^T$ and $\underline{\mu} = (\underline{\mu}_1, \underline{\mu}_2, ..., \underline{\mu}_m)^T$. And the symbol Ω denotes the set of branches in power systems with the cardinality $|\Omega| = n$ (i.e. the number of branches). Since the cost function is a convex function and the inequality constraints are affine, the above necessary condition is also sufficient for optimality. As we can see, System (4) in this document is composed of $(7m+6n)$ equations and $(7m+6n)$ additional unknown variables (i.e. P^l, $\underline{w}_{ij}$, $\bar{w}_{ij}$, $\underline{\lambda}_{ij}$, $\bar{\lambda}_{ij}$, $\underline{y}_{ij}$, $\bar{y}_{ij}$, $\underline{x}_i$, $\bar{x}_i$, $\underline{z}_i$, $\bar{z}_i$, $\underline{\mu}_i$, $\bar{\mu}_i$). Note that Y_b^l contains the existing unknown variables Y_p^l in the paper. By combining System (4) in this document with Equations (8) and (9) in the paper, we can obtain an extended system of algebraic equations with $7m+(6+h)n$ equations and $7m+(6+h)n$ unknown variables. The extended system of algebraic equations can be solved using the numerical solver (e.g. "fsolve" in Matlab). In this way, load shedding and generation control can be taken into account in the proposed optimal control formulation of identifying the worst-case cascading failures.

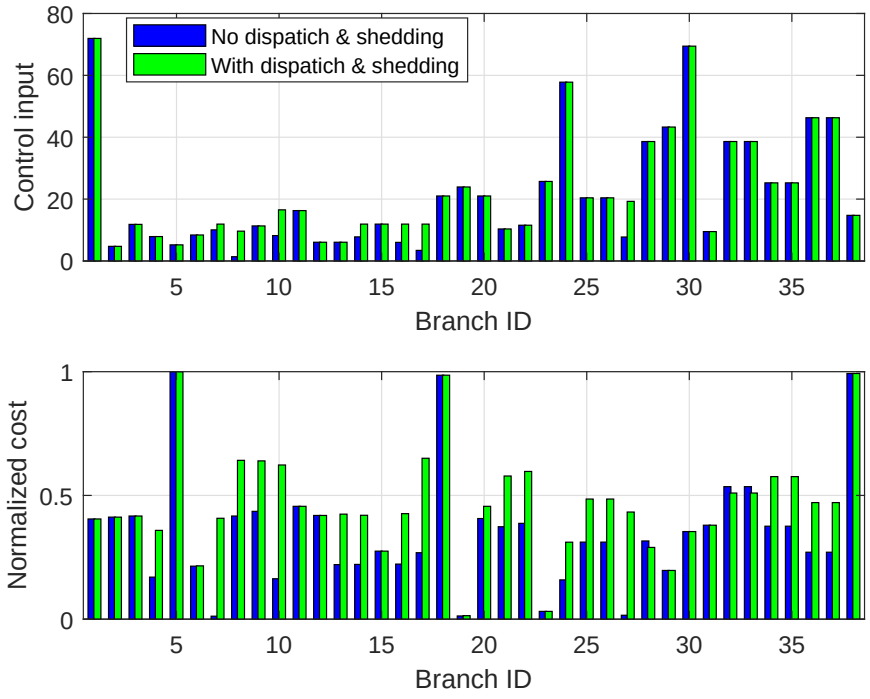

Figure 4: Control inputs and normalized costs of the cascades with and without generation dispatch and load shedding on the IEEE 24 Bus System.

To demonstrate the effectiveness of the above approach, numerical simulations are conducted on the IEEE 24 Bus System to identify the initial disturbance on each branch. The parameter setting is the same as that in the paper. The generation dispatch and load shedding are implemented at the 4-th cascading step (i.e. $l = 4$). Figure 4 presents the initial disturbances (i.e. control inputs) on each branch identified by the proposed optimal control approach and the resulting normalized costs to quantify the disruption level of cascades (i.e. the index γ in the paper, where a smaller γ indicates a worse cascades). Specifically, the blue bars denote the control inputs and normalized costs without generation dispatch and load shedding, while the green bars represent those with generation dispatch and load shedding. As we can observe in the upper panel of Figure 4, the height of green bar is not smaller than that of blue bar for each branch. This indicates that larger initial disturbances (i.e. the magnitude of control input) are required to trigger the worst-case cascades of power grids with generation dispatch and load shedding compared to those without generation dispatch and load shedding. It is worth pointing out that the branches with equal heights of blue bar and green bar (e.g. Branch 1, Branch 2, Branch 3, Branch 4, Branch 5, Branch 6, etc) are directly severed by the initial disturbances (i.e. control inputs). The lower panel of Figure 4 demonstrates that the cascades with generation dispatch and load shedding are less disruptive on the whole except for the cascades triggered by the initial disturbances on Branch 28, Branch 32 and Branch 33. This is because the optimal solutions for generation dispatch and load shedding are not available at the specified cascading step. Thus, the adjustment of injected power on buses (i.e. generation dispatch and load shedding) actually deteriorates branch overloads and results in the worse disruptions of cascades in the end.

References

[1] Song, J., Cotilla-Sanchez, E., Ghanavati, G. and Hines, P.D., 2016. Dynamic modeling of cascading failure in power systems. IEEE Transactions on Power Systems, 31(3), pp. 2085-2095.

[2] Fitzmaurice, R., Cotilla-Sanchez, E. and Hines, P., 2012, July. Evaluating the impact of modeling assumptions for cascading failure simulation. In 2012 IEEE Power and Energy

Society General Meeting, pp. 1-8.

[3] Van den Bergh, K., Delarue, E. and D'haeseleer, W., 2014. DC power flow in unit commitment models. TMF Working Paper-Energy and Environment, Tech. Rep.

[4] Carreras, B.A., Lynch, V.E., Dobson, I. and Newman, D.E., 2002. Critical points and transitions in an electric power transmission model for cascading failure blackouts. Chaos: An interdisciplinary journal of nonlinear science, 12(4), pp.985-994.